

Nod Factors Integrate Spontaneously in Biomembranes and Transfer Rapidly between Membranes and to Root Hairs, but Transbilayer Flip-Flop Does Not Occur[†]

Joachim Goedhart,[‡] Horst Röhrig,[§] Mark A. Hink,[‡] Arie van Hoek,[‡] Antonie J. W. G. Visser,[‡] Ton Bisseling,[‡] and Theodorus W. J. Gadella, Jr.*[‡]

MicroSpectroscopy Center Wageningen, Department of Biomolecular Sciences, Wageningen Agricultural University, Dreijenlaan 3, 6703 HA Wageningen, The Netherlands, and Abteilung Genetische Grundlagen der Pflanzenzüchtung, Max-Planck-Institut für Züchtungsforschung, D-50829 Köln, Federal Republic of Germany

Received March 26, 1999; Revised Manuscript Received June 15, 1999

ABSTRACT: Three novel nodulation (Nod) factors were synthesized from chitotetraose and three structurally different fluorescent BODIPY-tagged fatty acids. With fluorescence spectroscopic and microscopic techniques, the following aspects were studied: whether these amphiphilic molecules insert in membranes, whether they transfer between different membranes, and whether they are able to transfer from a membrane to a legume root hair. Fluorescence correlation spectroscopy showed that fluorescent Nod factors are present as monomers in PBS buffer at a concentration of 10 nM, but that when either Triton X-100 micelles or dioleoylphosphatidylcholine (DOPC) vesicles are present, the Nod factors are associated with these particles. With time-correlated single-photon counting fluorescence spectroscopy, it was shown that upon Nod factor insertion in the membrane, the rotation of the fluorescent acyl chain was markedly reduced. A fluorescence resonance energy transfer assay was used to study the transfer of Nod factors from one membrane to the other, or from vesicles to root hairs. Nod factors transfer rapidly between membranes or from vesicles to root hair cell walls. However, they do not flip-flop between membrane leaflets. The results provide novel insights for the mode of secretion and transfer of Nod factors during the early steps of the *Rhizobium*–legume interaction.

Nodulation (Nod)¹ factors are signal molecules secreted by Gram-negative *Rhizobium* bacteria and play a key role in the early steps of nodule formation (1, 2). Root nodules are the result of a *Rhizobium*–legume interaction. In these specialized organs, the rhizobia are intracellular and convert atmospheric nitrogen into ammonium. In exchange for sugars, the ammonium is fed to the plant. In the initial steps of the interaction, flavonoids secreted by the legume root

induce the expression of the *nod* genes of the bacterium, resulting in the production of Nod factors. The production and secretion of Nod factors is essential for all early steps of nodulation, and its chemical structure determines host specificity (3). All Nod factors comprise a chitin backbone of three to five β -1,4-linked *N*-acetylglucosamine residues. A fatty acyl chain of 16–20 carbon atoms with different degrees of unsaturation is N-linked to the nonreducing terminal sugar. Major determinants of host specificity are the decorations of the chitin backbone which can be acetate, sulfate, and fucosyl groups (4, 5).

Purified Nod factors, from *Rhizobium* cultures (5, 6) or synthesized (7, 8), are active at picomolar concentrations. They can induce root hair depolarization (9), root hair deformation (5, 10), cortical cell division (11), and primordium formation (12). To obtain more insight into the possible mechanisms of secretion and perception of Nod factors, it is necessary to study the molecular behavior of these peculiar amphiphilic molecules. Both in the secretion process by *Rhizobium* bacteria and during perception by root hairs of leguminous plants, membranes play an important role; two bacterial membranes have to be passed to accomplish secretion, and membrane-bound receptors have been postulated for Nod factor perception (13). Given the hydrophobic fatty acyl chain of the Nod factors, it is expected that Nod factors will have a high tendency to insert into membranes. Orgambide et al. (14) show that Nod factors are primarily present in rhizobial membranes. Furthermore, they also speculate that Nod factors diffuse as micelles through the

[†] This work was supported by a grant (to J.G. and M.A.H.) from the Netherlands Council of Earth- and Life Sciences (ALW) and by a grant (to T.W.J.G.) from the Royal Netherlands Academy of Arts and Sciences (KNAW). The collaboration with H.R. was supported by a EU-TMR program. The fluorescence correlation spectroscopy setup was made available by an investment grant of the Netherlands Organization for Scientific Research (NWO).

* Corresponding author. Telephone: +31 317 484284. Fax: +31 317 483584. E-mail: Dorus.Gadella@laser.bc.wau.nl.

[‡] Wageningen Agricultural University.

[§] Max-Planck-Institut für Züchtungsforschung.

¹ Abbreviations: BODIPY FL-C₁₆, 4,4-difluoro-5,7-dimethyl-4-bora-3a,4a-diaza-*s*-indacene-3-hexadecanoic acid; BODIPY 558/568-C₁₂, 4,4-difluoro-5-(2-thienyl)-4-bora-3a,4a-diaza-*s*-indacene-3-dodecanoic acid; BODIPY 581/591-C₁₁, 4,4-difluoro-5-(4-phenyl-1,3-butadienyl)-4-bora-3a,4a-diaza-*s*-indacene-3-undecanoic acid; BODIPY 581/591-C₁₆, 4,4-difluoro-5-(4-phenyl-1,3-butadienyl)-4-bora-3a,4a-diaza-*s*-indacene-3-hexadecanoic acid; DHPE, 1,2-dihexadecanoyl-*sn*-glycero-3-phosphoethanolamine; DMSO, dimethyl sulfoxide; DOPC, 1,2-dioleoyl-*sn*-glycero-3-phosphocholine; DPPA, 1,2-dipalmitoyl-*sn*-glycero-3-phosphate; FCS, fluorescence correlation spectroscopy; FRET, fluorescence resonance energy transfer; NBD, 7-nitrobenz-2-oxa-1,3-diazole; Nod factor, nodulation factor; NodRlv-IV, tetrameric Nodulation factors from *Rhizobium leguminosarum* bv. *viciae*; PBS, phosphate-buffered saline; PGM, plant growth medium; TCSPC, time-correlated single-photon counting.

aqueous phase. However, no evidence for this concept is available as no detailed studies on the physicochemical properties of Nod factors have been reported so far.

Recently, the synthesis of fluorescent Nod factor derivatives via attachment of a BODIPY fluorophore to the acyl chain has been described (8). The labeled molecules enable the characterization of molecular behavior of these amphiphilic molecules by fluorescence spectroscopic and microscopic techniques. A relatively new technique based on the confocal principle, fluorescence correlation spectroscopy (FCS), was used to study the molecular diffusion rates and aggregation state of the fluorescent Nod factors. With FCS, fluorescence intensity fluctuations due to the movement of fluorescent molecules in and out the confocal volume element are assessed. Via correlation of these fluctuations over time, quantitative information about the mobility and local concentration of fluorescent probes can be obtained (15, 16).

We have synthesized three novel fluorescent Nod factors with different acyl chains, containing red-shifted BODIPY fluorophores. We focus on the molecular behavior of fluorescent Nod factors in the presence and absence of artificial membranes. Both steady state and time-resolved fluorescence spectroscopy were used to report on the molecular environment of the fluorescent tag of the Nod factors. We studied the mode of incorporation of Nod factors in model membranes, their ability to flip-flop between membrane leaflets, and their ability to diffuse from one membrane to another or from membranes to root hair cell walls. The implications for both Nod factor secretion and transfer during the early steps of the *Rhizobium*–legume interaction are discussed.

MATERIALS AND METHODS

Materials. All fluorescent probes, except for erythrosine B (Eastman Kodak, Rochester, NY), were purchased from Molecular Probes Europe (Leiden, The Netherlands). BODIPY 581/591- C_{16} was a Molecular Probes custom synthesis product. Triton X-100 (for gas chromatography), ethanol, and DMSO (spectroscopic grade) were from Merck (Darmstadt, Germany). DOPC, the sodium salt of DPPA, and mannitol (plant cell culture tested) were from Sigma (Zwijndrecht, The Netherlands). To make DPPA soluble in ethanol, DPPA was converted to the acid form by acidic extraction by dissolving in $CHCl_3/CH_3OH/0.6$ M HCl (1:2:0.8 v/v), phase separation by addition of $1/4$ of a volume of H_2O and $CHCl_3$, and subsequent evaporation of the isolated lower phase (17).

Fluorescent Nod Factors. The synthesis of NodRlv-IV (BODIPY FL- C_{16}) is described in ref 8. Correspondingly, three novel Nod factors differing in both acyl chain length and fluorophore structure are synthesized and purified. According to the nomenclature proposed by Roche et al. (3), the Nod factors are denoted as NodRlv-IV(BODIPY 558/568- C_{12}), NodRlv-IV(BODIPY 581/591- C_{11}), and NodRlv-IV(BODIPY 581/591- C_{16}).

Plant Material. Seeds of *Vicia sativa* ssp. *nigra* were germinated and grown in modified Fåhrens slides (18) as described previously (10, 19). The plant growth medium (PGM) was composed of 2.72 mM $CaCl_2$, 1.95 mM $MgSO_4$, 2.20 mM KH_2PO_4 , 1.26 mM Na_2HPO_4 , and 0.08 mM Fe(III) citrate. Root hair deformation assays were carried out

as described previously (10). DMSO and ethanol concentrations were never higher than 0.1% (v/v).

Fluorescence Spectroscopy. Nod factors were dissolved in ethanol and pipetted in 1 mL quartz cuvettes. All excitation and emission spectra were recorded on a SPF-500C spectrofluorimeter (SLM instruments, Urbana, IL). Excitation spectra were recorded by monitoring emission (slit width of 5 nm) at 560, 610, and 650 nm and scanning excitation (slit width of 2 nm) from 400 to 550, 450 to 600, and 500 to 630 nm for BODIPY FL, BODIPY 558/568, and BODIPY 581/591, respectively. Emission spectra were recorded by excitation (slit width of 5 nm) at 450, 500, and 520 nm and scanning emission (slit width of 2 nm) from 460 to 600, 510 to 650, and 530 to 570 nm for BODIPY FL, BODIPY 558/568, and BODIPY 581/591, respectively.

Preparation of Micelles and Vesicles. Phosphate-buffered saline (PBS) consisted of 10 mM phosphate (pH 7.4) and 154 mM NaCl. Triton X-100 was added to a final concentration of 0.2% in PBS (v/v) to obtain micelles. Small unilamellar vesicles were made as described previously (20) by injecting 10 μ L of a solution of DOPC in ethanol into 1 mL of PBS, to yield a final DOPC concentration of 50 μ M. The fluorescent Nod factors were added from DMSO stock solutions to PBS, Triton X-100 micelles, or DOPC vesicles to a final Nod factor concentration of 10 nM.

For transfer experiments, donor vesicles were made as described above, by injecting 20 μ L of an ethanolic solution of 790 μ M DOPC, 100 μ M DPPA, 10 μ M NodRlv-IV (BODIPY FL- C_{16}) or 10 μ M BODIPY 530/550 DHPE, and 100 μ M Texas Red DHPE into 3 mL of Tris buffer [20 mM Tris (pH 7.4), 100 mM NaCl, 1 mM EDTA, and 1 mM EGTA], under continuous stirring. Alternatively, the ethanolic solution was evaporated, and 3 mL of Tris buffer was added followed by sonication using a Branson tip sonifier (Danbury, CT) for 3 min with an output power of 15 W (30% duty cycle). Acceptor vesicles were prepared by mixing 3600 nmol of DOPC and 400 nmol of DPPA in chloroform. After evaporation of the chloroform, the lipids were dissolved in 2 mL of Tris buffer by vortexing, followed by sonication for 3 min. To monitor transfer from vesicles to roots, donor vesicles prepared by sonication consisted of 80 μ M DOPC, 10 μ M DPPA, 10 μ M Texas Red DHPE, and 0.6 μ M NodRlv-IV(BODIPY FL- C_{16}) or 0.6 μ M BODIPY FL DHPE (final concentrations in PGM without calcium).

Nod Factor Transfer Assay. The emission of NodRlv-IV (BODIPY FL- C_{16}) was monitored continuously on an Aminco SLM-8000 (SLM instruments, Urbana, IL) by excitation at 490 nm (slit width of 4 nm) and emission at 513 or 550 nm (slit width of 4 nm). To start the assay, 100 μ L of acceptor vesicles was added to 3 mL of donor vesicles, and the fluorescence intensity was monitored as a function of time. For calibration, aliquots of 25 μ L of 10% (v/v) Triton X-100 in PBS were added, until the fluorescence intensity did not increase.

Fluorescence Microscopy. Fluorescence microscopy was performed with the FRIM system described by Gadella et al. (8) based on a Leica DMR microscope (Leitz, Wetzlar, Germany) with Leitz fluotar 10 \times NA 0.3 air or fluotar 40 \times NA 0.5–1.0 oil immersion objectives. In addition to the CH250 CCD camera, images were captured by a Quantix CCD camera (Photometrics, Tucson, AZ) interfaced through a PCI card with an Apple Macintosh PowerPC 8500/180

computer (Apple Computer, Cupertino, CA) and controlled by IPLab 3.1 software (Signal Analytics, Vienna, VA). The fluorescence of BODIPY FL was acquired by excitation with a 100 W USH-102D mercury lamp (Fairlight, Rotterdam, The Netherlands) and an Omega (Omega Optical, Brattleboro, VT) 490DF20 band-pass filter. The emission was separated by an Omega 505 DRLP dichroic mirror and passed through a 525DF30 band-pass filter.

Fluorescence Correlation Spectroscopy. FCS measurements were performed with a Zeiss-EVOTEC ConfoCor instrument (Carl-Zeiss, Jena, Germany, and Evotec Biosystems, Hamburg, Germany). Briefly, the system consists of a Zeiss inverted confocal microscope, and uses either an air-cooled argon ion laser (488 nm) or a helium–neon laser (543 nm) for excitation. Standard confocal epifluorescence microscope optics are used, including dichroic mirrors (510 or 560 nm for the respective laser lines), a Zeiss water immersion objective (C-Apochromat 40 \times , 1.2 NA, 440052), and band-pass filters for selecting the fluorescence emission (515–565 or 565–610 nm for the respective laser lines). The emission was spatially filtered through a pinhole (diameter of 40 μm) and detected by an avalanche photodiode coupled to a fast digital correlator. Data acquisition and analysis were performed using the FCS ACCESS software package (EVOTEC/Zeiss, Inc., version 1.0.12) running under Windows95 (Microsoft, Inc.). The system is described in detail elsewhere (21, 22). Samples were measured, and calibration (see below) was performed in eight-chamber coverglasses (Nalge Nunc International, Naperville, IL) having a borosilicate bottom with a thickness of 0.135 mm. The laser beam was focused 150 μm above the bottom of the chamber. Acquisition times for calibration and samples were 30–60 s. All experiments were carried out at room temperature.

Calibration was done with rhodamine green in H₂O for 488 nm excitation and with tetramethylrhodamine or tetramethylrhodaminedextran (MW of 10 000) in H₂O for 543 nm excitation, which have known diffusion constants of 2.8×10^{-10} , 2.8×10^{-10} , and 1.36×10^{-10} m² s⁻¹, respectively (23). The triplet time constant was fixed to 5 μs during evaluation of the calibration results because of the use of air-saturated solutions. From these results, the axial radii of the laser beam at the focal plane, ω_1 , with excitation at 488 and 543 nm were calculated, which were 0.30 and 0.36 μm , respectively. The diffusion constants are related to diffusion times according to eq 1 (21):

$$\tau = \frac{\omega_1^2}{4D} \quad (1)$$

in which τ is the diffusion time in seconds and D is the diffusion constant in square meters per second. The volume, V , of the confocal element (cubic meters) can be calculated from the axial laser radius ω_1 and structural parameter (SP) obtained from the calibration (21):

$$V = 2\pi\omega_1^3 \text{SP} \quad (2)$$

The radius, r , of spherical particles is related to the diffusion constant via the Stokes–Einstein equation (24):

$$r = \frac{kT}{6\pi\eta D} = \sqrt[3]{\frac{3kT\phi}{4\pi\eta}} \quad (3)$$

For the viscosity, η , the value of water is taken to be 10^{-3} kg m⁻¹ s⁻¹, T is the absolute temperature, ϕ is the rotational correlation time obtained by anisotropy decay analysis, and k is the Boltzmann constant.

Time-Correlated Single-Photon Counting. Time-resolved experiments were carried out on the TCSPC setup as described in detail previously (25, 26). The excitation wavelength was 510 nm (coumarin 460 dye as the laser medium, pumped by a mode-locked Nd:YLF laser), and emission was detected using a Schott (Mainz, Germany) OG 530 nm cutoff and Balzers Filtraflex K55 band-pass filter (Balzers, Liechtenstein) for BODIPY FL emission, a Schott 570.3 nm band-pass filter for BODIPY 558/568 emission, or a Schott KV 550 nm cutoff and an Omega 580DF30 nm band-pass filter for BODIPY 581/591 emission. For each decay, 1024 channels were collected with a time spacing of 25 ps. Ten to twenty cycles were acquired for the sample, three cycles for the reference, and two to eight for the blank, depending on the signal intensity. Erythrosine B in H₂O ($\text{OD}_{\text{max}} < 0.1$), with a known single lifetime of 80 ps, was used as a reference for deconvoluting the instrumental response function. Total fluorescence decay and fluorescence anisotropy decay experiments were analyzed according to a multiexponential decay law using a global analysis program, the principle of which has been described previously (27) and is based on a Marquardt nonlinear least-squares procedure (28). The complete anisotropy decays were analyzed, and χ^2 values were calculated starting from channel 25, at which the fluorescence reached the maximal intensity. The 67% confidence limits of the rotational correlation times were determined by a rigorous error analysis (27).

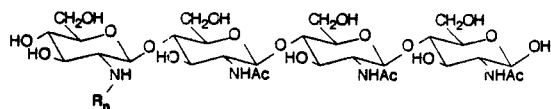
RESULTS

Synthesis and Spectral Properties of Fluorescent Nod Factors. The fluorescent Nod factor derivatives are synthesized by N-acylation of the amino group at the nonreducing end of NodB-treated chitotetraose with BODIPY-labeled fatty acids and purified on reversed phase HPLC as described previously (8). The structures of the synthesized Nod factors are shown in Figure 1A. Fluorescence emission and excitation spectra of the Nod factors were recorded to evaluate the spectral properties. In Figure 1B, the normalized excitation and emission spectra of NodRlv-IV(BODIPY FL-C₁₆), NodRlv-IV(BODIPY 558/568-C₁₂), and NodRlv-IV(BODIPY 581/591-C₁₆) in ethanol are presented, showing a small difference between excitation and emission maximum (Stokes shift) and narrow spectral bandwidth, typical for BODIPY (29). The excitation and emission spectra of NodRlv-IV(BODIPY 581/591-C₁₆) were identical to the spectra of NodRlv-IV(BODIPY 581/591-C₁₁). The Nod factors labeled with BODIPY 581/591 have superior spectral properties compared to Nod factors labeled with BODIPY FL (8) or NBD (30), because of (i) their very high extinction coefficients (150 000 M⁻¹ cm⁻¹), (ii) their high fluorescence quantum yields (about 0.9), (iii) the low sensitivity to the environment (31), and (iv) favorable excitation and emission wavelengths with respect to root autofluorescence (8).

The Bioactivity of Nod Factors Depends on Acyl Chain Structures. The bioactivity of the different fluorescent Nod

A

Chitin Backbone:



Fatty acyl chain:

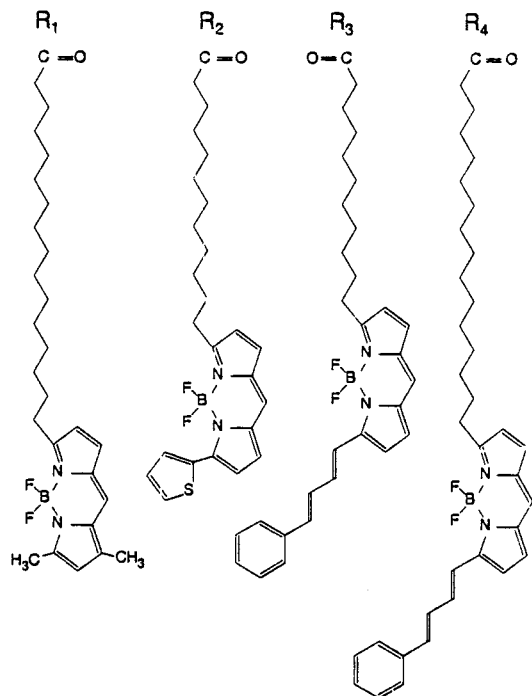
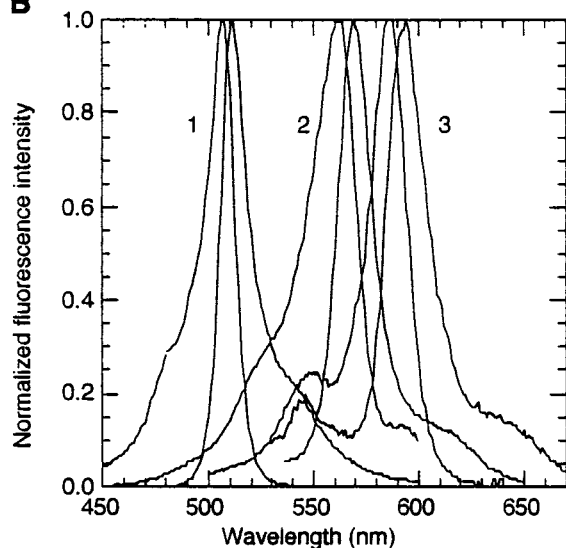
**B**

FIGURE 1: Structure and spectral properties of the four fluorescent Nod factors used in this study. (A) Chitin backbone and fatty acyl chain structure of the fluorescent Nod factors. The chitin backbone consists of four β -1,4-linked N-acetylated glucosamine residues, as for Nod factors secreted by *Rhizobium leguminosarum* bv. *viciae*. The four different fatty acyl chains attached to the nonreducing end carrying the fluorophore are BODIPY FL-C₁₆ (R₁), BODIPY 558/568-C₁₂ (R₂), BODIPY 581/591-C₁₁ (R₃), and BODIPY 581/591-C₁₆ (R₄). (B) Normalized fluorescence excitation and emission spectra of NodRlv-IV(BODIPY FL-C₁₆) (1), NodRlv-IV(BODIPY 558/568-C₁₂) (2), and NodRlv-IV(BODIPY 581/591-C₁₆) (3) recorded in ethanol. The excitation and emission spectra of NodRlv-IV(BODIPY 581/591-C₁₁) were similar to spectra 3.

Table 1: Bioactivity of the Fluorescent Nod Factors in the Root Hair Deformation Assay

acyl chain ^a	10 ⁻⁶ mol/L	10 ⁻⁷ mol/L	10 ⁻⁸ mol/L	10 ⁻⁹ mol/L	10 ⁻¹⁰ mol/L	10 ⁻¹¹ mol/L
BODIPY FL-C ₁₆	+ ^b	+	+	± ^c	- ^d	nd ^e
BODIPY 558/568-C ₁₂	nd	+	±	-	nd	nd
BODIPY 581/591-C ₁₁	nd	-	-	-	nd	nd
BODIPY 581/591-C ₁₆	nd	nd	+	+	+	-

^a Type of acyl chain attached to the chitin backbone; see Figure 1A.

^b Significant deformation in the susceptible zone. ^c Reduced level of deformation in the susceptible zone. ^d No deformation. ^e Not determined.

factors was tested in a root hair deformation assay. As shown in Table 1, NodRlv-IV(BODIPY 581/591-C₁₆) exhibits root hair deformation at concentrations as low as 10⁻¹⁰ M, approaching the bioactivity of natural Nod factors (10). This clearly shows that the presence of the relatively bulky BODIPY moiety does not abolish the biological response, as was noted previously also for the second best Nod factor with the BODIPY FL-C₁₆ acyl chain which exhibits activity down to 10⁻⁹ M. It is very remarkable that a Nod factor also labeled with BODIPY 581/591 but with an acyl chain that is five carbon atoms shorter [NodRlv-IV (BODIPY 581/591-C₁₁)] was found to be completely incapable of inducing root hair deformation even at 10⁻⁷ M. The BODIPY 558/568-C₁₂-labeled Nod factor loses activity at concentrations lower than 10⁻⁸ M in the deformation assay. Our data do not show a clear relationship between bioactivity and Nod factor acyl chain hydrophobicity since NodRlv-IV(BODIPY FL-C₁₆), NodRlv-IV(BODIPY 558/568-C₁₂), and NodRlv-IV(BODIPY 581/591-C₁₁) have quite similar hydrophobicities, but differ remarkably in their bioactivities. Apparently, bulky substitutions at the C₁₁ position of the acyl chain abolish bioactivity. On the other hand, even large hydrophobic modifications at the very end (beyond C₁₅) of the acyl chain do not seem to interfere with perception. We speculate that this ambiguous structure-response relation could reflect structural features of a fatty acyl binding pocket of the putative Nod factor receptor.

FCS on Fluorescent Nod Factors in the Presence and Absence of Artificial Membranes. The amphiphilic nature of Nod factors suggests that they will readily incorporate into membranes. To study the association of the Nod factors with membranes, we studied the diffusional behavior of fluorescent Nod factors in the presence and absence of micelles or phospholipid vesicles by FCS. Upon incorporation into micelles or vesicles, the diffusion rate of Nod factors will be markedly reduced and will correspond to the diffusion rate of these membrane-like structures.

In Figure 2A, the autocorrelation functions obtained by FCS with NodRlv-IV(BODIPY FL-C₁₆) in different environments are shown. In PBS, the correlation of signal fluctuations rapidly decreases at time intervals larger than about 100 μ s. From the curve fit of the correlation curves, average diffusion times for the different Nod factors were determined, ranging from 84 to 127 μ s. Using the average diffusion time, and the radius of the laser focus, the diffusion constant can be calculated according to eq 1, giving a value of 2.68×10^{-10} m² s⁻¹ for NodRlv-IV(BODIPY FL-C₁₆). This diffusion constant implies a particle with a hydrodynamic radius of 0.80 nm according to eq 3 and therefore reflects diffusion of Nod factor monomers. When NodRlv-IV(BODIPY FL-

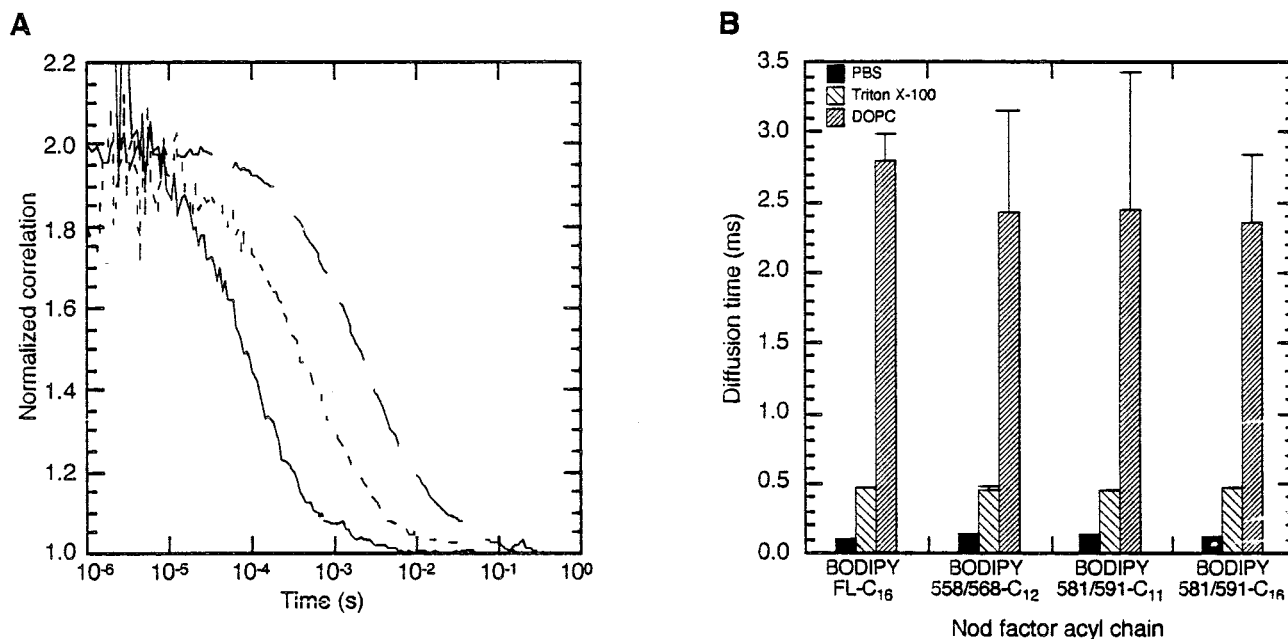


FIGURE 2: Fluorescence correlation spectroscopy of Nod factors in different environments. (A) Normalized autocorrelation functions of NodRlv-IV(BODIPY FL-C₁₆). The experiments were all carried out with 10 nM Nod factor added to a solution of PBS (—), micelles [0.2% (v/v) Triton X-100] (---), or vesicles (50 μ M DOPC) (---). (B) Diffusion times of the four fluorescent Nod factors. Nod factors were added to PBS, 0.2% (v/v) Triton X-100, or 50 μ M DOPC. The Nod factor concentration was 10 nM, and the diffusion times presented in this figure are the average of five measurements.

C₁₆) is added to a micelle solution, the diffusional mobility decreases considerably, as can be seen in Figure 2A from the shift of the autocorrelation curve to longer diffusion times. Analysis of the curve yields diffusion times of around 450 μ s, representing the lateral mobility of Triton X-100 micelles (21). When Nod factors were studied in the presence of small unilamellar vesicles of DOPC, the diffusion times were increased further. Curve analysis revealed relatively heterogeneous diffusional behavior, with an average diffusion time of 2.4 ms (Figure 2B). Similar diffusion times were measured for vesicles in which phospholipids with a BODIPY-labeled acyl chain were incorporated (21). This indicates that also in the presence of vesicles, Nod factors incorporate into the vesicles and diffuse with a corresponding slower rate.

In Figure 2B, the average diffusion times determined from the autocorrelation functions of the four fluorescent Nod factors are presented. From this figure, it is clear that the diffusion times of the different Nod factors are very similar if they are in the same environment. Regardless of the acyl chain structure, all four Nod factors at a concentration of 10 nM diffuse as monomers in aqueous solution, but in the presence of micelles or phospholipid vesicles, the Nod factors associate completely with these structures and diffuse with corresponding rates, irrespective of the differences in the Nod factor acyl chain.

TCSPC of Fluorescent Nod Factors in Different Environments. To study whether upon association with vesicles or micelles the acyl chain of the Nod factor is inserted into the lipid core of these structures, we investigated the rotational mobility of the Nod factor acyl chain in the presence and absence of vesicles and micelles. The rotational mobility of fluorophores can be investigated with TCSPC spectroscopy. A short (picosecond duration) pulse of laser light is used to excite the sample, and the intensity and anisotropy of the fluorescence can be monitored as a function of time

(nanosecond time scale). In Figure 3A, the experimental anisotropy decay curves for NodRlv-IV(BODIPY FL-C₁₆) in the presence of DOPC vesicles, Triton X-100 micelles, or only PBS are shown. From the curvature in the logarithmic plots, it can be inferred that the decays are multiexponential. The anisotropy decays in the presence of micelles or vesicles are quite similar. However, the decay of NodRlv-IV(BODIPY FL-C₁₆) in only PBS is much faster, indicating large differences in the rotational freedom of the acyl chain.

The experimental curves were analyzed to obtain the parameters describing the decay, the rotational correlation times ϕ , and their contribution β (see Table 2). In some cases, a limiting anisotropy, of which the contribution β_{∞} was analyzed, was included. The theoretical decays of NodRlv-IV(BODIPY FL-C₁₆) constructed from the parameters of the analysis are shown in Figure 3A as smooth lines. The residuals are randomly scattered around zero (Figure 3B), indicating an accurate fit of the data.

In PBS, NodRlv-IV(BODIPY FL-C₁₆) exhibits two short rotational correlation times. The longer time ϕ_2 , 0.50 ns, corresponds with motions of the whole molecule, whereas the shorter and predominant time ϕ_1 probably reflects an independent rotational motion of the BODIPY moiety. A limiting anisotropy with a very small contribution β_{∞} is present (3% of r_0), likely reflecting Nod factors adsorbed on the cuvette. According to the Stokes–Einstein relation (eq 3), the rotational correlation time ϕ_2 corresponds to a hydrodynamic radius of 0.78 nm, indicating that the Nod factors are present as monomers. This agrees very well with the hydrodynamic radius that was calculated from FCS measurements of Nod factors in buffer.

When NodRlv-IV(BODIPY FL-C₁₆) is studied in the presence of micelles or DOPC, the very short rotational correlation time disappears, and two longer times appear (see Table 2). The absence of the very short correlation times and the presence of longer correlation times show that the

Table 2: Anisotropy Decay Parameters of the Four Fluorescent Nod Factors in Different Environments

acyl chain ^a	solvent	β_1	ϕ_1 (ns)	β_2	ϕ_2 (ns)	β_∞	r_0^b	χ^2
BODIPY FL-C ₁₆	PBS	0.22 (0.10–0.37) ^c	0.07 (0.02–0.16)	0.07 (0.02–0.13)	0.50 (0.31–1.50)	0.008 (0.005–0.010)	0.30	1.48
BODIPY 558/568-C ₁₂	PBS			0.29 (0.18–0.31)	0.24 (0.21–0.56)	0.012 (0.008–0.015)	0.30	1.27
BODIPY 581/591-C ₁₁	PBS			0.29 (0.20–0.31)	0.39 (0.34–0.54)		0.29	1.25
BODIPY 581/591-C ₁₆	PBS			0.25 (0.17–0.33)	0.46 (0.33–0.75)		0.25	1.19
BODIPY FL-C ₁₆	Triton	0.17 (0.13–0.21)	1.19 (0.79–1.66)	0.19 (0.14–0.23)	6.23 (5.23–8.09)		0.35	1.31
BODIPY 558/568-C ₁₂	Triton	0.14 (0.10–0.20)	1.33 (0.80–2.22)	0.20 (0.13–0.25)	6.82 (5.72–9.94)		0.34	1.26
BODIPY 581/591-C ₁₁	Triton	0.20 (0.18–0.23)	4.97 (4.08–5.83)	0.12 (0.09–0.14)	25 ^d		0.32	1.21
BODIPY 581/591-C ₁₆	Triton	0.18 (0.15–0.22)	5.00 (3.91–7.14)	0.14 (0.08–0.16)	25 ^d		0.31	1.24
BODIPY FL-C ₁₆	DOPC	0.17 (0.13–0.20)	0.72 (0.52–1.06)	0.15 (0.11–0.18)	4.32 (3.25–7.06)	0.017 (0.003–0.026)	0.34	1.31
BODIPY 558/568-C ₁₂	DOPC	0.16 (0.13–0.18)	0.85 (0.59–1.19)	0.16 (0.13–0.18)	7.81 (6.63–9.71)		0.32	1.33
BODIPY 581/591-C ₁₁	DOPC	0.08 (0.06–0.11)	0.78 (0.40–1.22)	0.22 (0.20–0.24)	7.04 (5.34–10.7)	0.050 (0.009–0.067)	0.34	1.39
BODIPY 581/591-C ₁₆	DOPC			0.21 (0.20–0.23)	5.83 (4.95–7.04)	0.082 (0.063–0.097)	0.29	1.24

^a Type of acyl chain attached to the chitin backbone; see Figure 1A. ^b Initial anisotropy = $\beta_1 + \beta_2 + \beta_\infty$. ^c Values in parentheses denote 67% confidence limits. ^d Fixed value, corresponding to micellar rotation calculated from FCS measurements (eq 3).

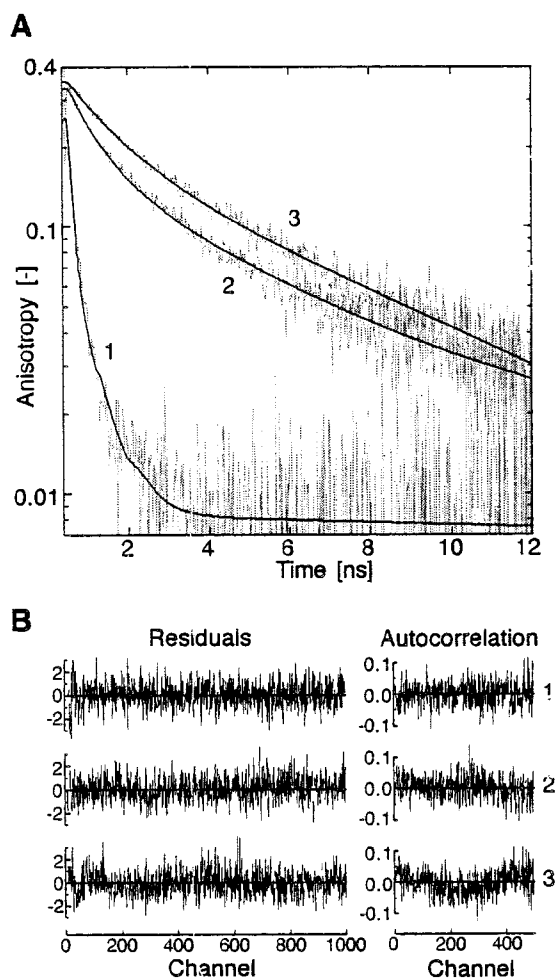


FIGURE 3: Anisotropy decays of 10 nM NodRlv-IV(BODIPY FL-C₁₆) in different environments. The data that are shown are representative of three experiments. (A) Experimental anisotropy decays of NodRlv-IV(BODIPY FL-C₁₆) in PBS (1), Triton X-100 micelles (2), or DOPC vesicles (3) and anisotropy decays calculated from the parameters listed in Table 2. (B) Residuals and autocorrelation curves depicting the quality of the fits.

rotational mobility of the Nod factor acyl chain is clearly decreased. The rotational correlation times observed in the presence of micelles represent wobbling (ϕ_1) and translational diffusion (ϕ_2) commonly observed in micellar systems (22). The two rotational correlation times of NodRlv-IV(BODIPY FL-C₁₆) in DOPC are comparable to the rotational correlation times of phosphatidylcholine with a BODIPY-labeled acyl chain, incorporated in DOPC vesicles (data not shown).

Hence, the decreased BODIPY rotational mobility reflects an insertion of the fluorescent acyl chain of the Nod factor deeply into the hydrophobic core of the micelle or in the lipid bilayer.

As can be inferred from Table 2, the other fluorescent Nod factors yield results similar to those obtained with NodRlv-IV(BODIPY FL-C₁₆). When Nod factors carrying an acyl chain with the BODIPY 581/591 fluorophore are inserted into micelles, translational diffusion as well as the rotation of the complete micelle ($\phi \approx 25$ ns) was observed, as has been described for fluorescent phospholipids in the presence of Triton X-100 micelles (22). Additionally, these Nod factors exhibit a relatively large limiting anisotropy (15–28% of r_0) when inserted in the vesicles, due to the relatively large fluorophore. The limiting anisotropy has also been described for other fluorescent molecules in membrane systems and reflects rotational mobility in a confined geometry or cone (32, 33).

Transfer of Fluorescent Nod Factors between Membranes. Given the marked preference of Nod factors to incorporate into membranes, we studied whether Nod factors are able to spontaneously leave one membrane and then insert into another membrane or whether they are unable to redistribute between different membranes. Both options would have direct implications for Nod factor-secretion mechanisms occurring in *Rhizobium* bacteria. We developed an assay based on assays for monitoring intermembrane phospholipid exchange (34–36). In short, fluorescent lipids (i.e., Nod factors) are incorporated into so-called donor vesicles. By employing fluorescence resonance energy transfer (FRET), the fluorescence of the lipids in the donor vesicles is quenched. Subsequently, an excess of unlabeled acceptor vesicles is added. Upon transfer of the fluorescent lipid from the quenched donor vesicle to an (unquenched) acceptor vesicle, the fluorescence intensity increases, which can be monitored over time.

In addition to NodRlv-IV(BODIPY FL-C₁₆), we incorporated nonexchangeable Texas Red DHPE as a FRET acceptor in the donor vesicles to effectively quench the Nod factor fluorescence. Consequently, the NodRlv-IV(BODIPY FL-C₁₆) fluorescence of the donor vesicles was very low, as shown in Figure 4A. Similar results were obtained for donor vesicles prepared with the ethanol injection method or with the sonication method (see Materials and Methods).

The addition of a 10-fold excess of acceptor vesicles to the sample resulted in a very rapid increase of the fluores-

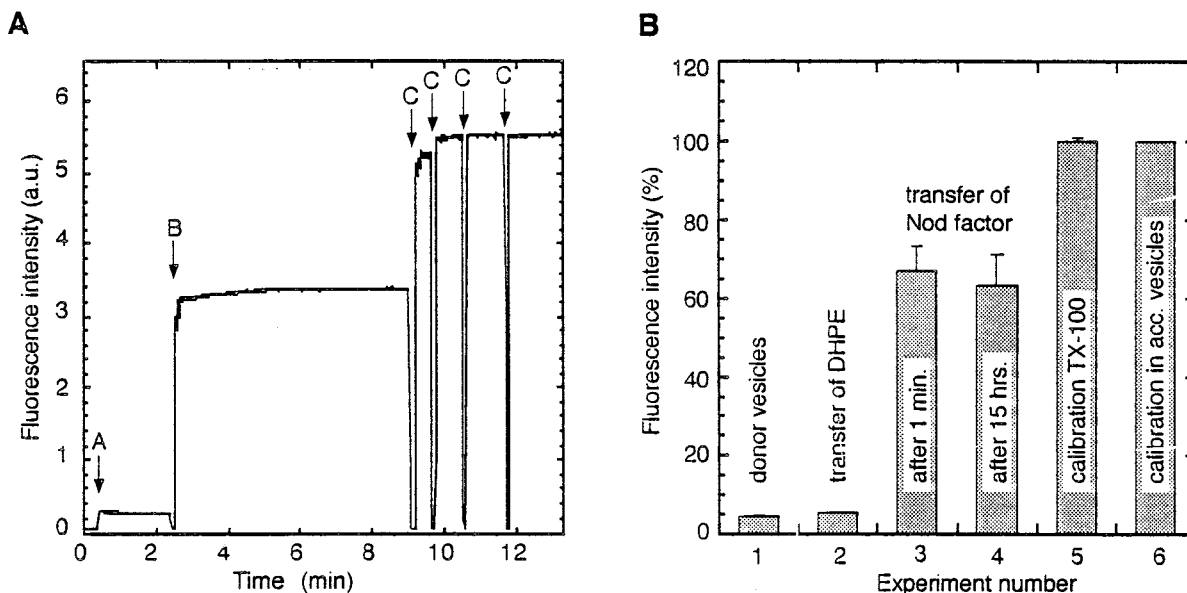


FIGURE 4: Intermembrane transfer of NodRlv-IV(BODIPY FL-C₁₆) from quenched donor to unquenched acceptor vesicles. (A) The fluorescence intensity of NodRlv-IV(BODIPY FL-C₁₆) is measured in arbitrary units (a.u.). At the arrow denoted with A, donor vesicles are generated by injection of an ethanolic solution [containing 79:10:10:1 DOPC/DPPA/Texas Red DHPE/NodRlv-IV(BODIPY FL-C₁₆), 20 nmol of total lipid] into 3 mL of Tris buffer under continuous stirring. For initiating spontaneous transfer, a 10-fold excess of acceptor vesicles (containing 90:10 DOPC/DPPA) was added at the arrow denoted with B. After four subsequent additions of 25 μ L of 10% (v/v) Triton X-100 in PBS (arrow denoted with C), the vesicles are completely solubilized, thereby dispersing and unquenching NodRlv-IV(BODIPY FL-C₁₆). (B) Normalized fluorescence intensity under various conditions. (1) Intensity obtained after preparing donor vesicles [79:10:10:1 DOPC/DPPA/Texas Red DHPE/NodRlv-IV(BODIPY FL-C₁₆), 20 nmol of total lipid in 3 mL of Tris] ($n = 4$). (2) Intensity obtained after adding acceptor vesicles to donor vesicles containing, instead of NodRlv-IV(BODIPY FL-C₁₆), the phospholipid BODIPY 530/550 DHPE ($n = 2$). (3) Fluorescence intensity observed after the addition of a 10-fold excess of acceptor vesicles to the donor vesicles prepared according to the conditions described for experiment 1 ($n = 4$). (4) Fluorescence intensity observed if the mixture described for experiment 3 is incubated for an additional 15 h ($n = 2$). (5) Emission after unquenching donor vesicles by solubilizing with 100 μ L of 10% (v/v) Triton X-100 ($n = 4$). (6) Fluorescence intensity of 200 nmol of unquenched acceptor vesicles consisting of 89.5:9.5:1 DOPC/DPPA/NodRlv-IV(BODIPY FL-C₁₆) in 3 mL of Tris. This signal represents a 100% transfer situation, is equal to the signal from experiment 5, and validates the calibration by solubilization with 100 μ L of 10% (v/v) Triton X-100 ($n = 3$).

cence intensity quickly reaching a constant level, indicating the rapid transfer of a substantial amount of NodRlv-IV(BODIPY FL-C₁₆) to the acceptor vesicles (Figure 4A). Again, no significant differences were observed for the different donor vesicle preparations (i.e., ethanol injection vs sonication). This indicates that the tiny amount of ethanol present after the ethanol injection [0.7% (v/v)] does not affect the transfer rate. After equilibrium was achieved, Triton X-100 was added (arrow C) to disperse and thereby unquench any Nod factors remaining in the donor vesicles. A further fluorescence increase (30–40%) was observed, indicating that in the equilibrium situation, about one-third of the NodRlv-IV(BODIPY FL-C₁₆) remained (quenched) in the donor vesicles. As for a control experiment, we incorporated the nontransferrable BODIPY 530/550 DHPE instead of fluorescent Nod factor into the donor vesicles. Also for these donor vesicles, the fluorescence intensity in buffer was low. After addition of acceptor vesicles, no increase in fluorescence was observed (see Figure 4B). This experiment confirms that BODIPY 530/550 DHPE does not spontaneously transfer between membranes as was also shown for other phosphatidylethanolamines (35). Moreover, it rules out alternative explanations of the fluorescence increase shown in Figure 4A at arrow B since (i) under the conditions used, Texas Red DHPE (used as a quencher) cannot transfer to acceptor vesicles, (ii) no fusion of the vesicles is detectable, and (iii) the acceptor vesicles have no fluorescence.

The experiment whose results are depicted in Figure 4A indicates that despite their distinct preference for membranes,

Nod factors rapidly equilibrate between different membranes. Similar observations have been made for lipids with a bulky polar headgroup and relatively low total hydrophobicity (i.e., phospholipids with short fatty acyl chains) (37). The critical transition for intermembrane transfer is the energy required for desorption of a lipid monomer from the membrane surface (38, 39). Obviously, the chitin moiety of the Nod factor provides ample opportunities for hydrogen bonding in the aqueous phase, thereby lowering the activation energy for Nod factor desorption and subsequent spontaneous monomeric transfer.

The average percentage of transferred NodRlv-IV(BODIPY FL-C₁₆) varied between 60 and 70% in several experiments, which corresponds well with the relative surface of the outer leaflet of small unilamellar vesicles (36, 40, 41). Hence, the immobile fraction reflects the Nod factor population trapped in the inner leaflet of the donor vesicles. Even 15 h after mixing of the donor and acceptor vesicles, no further increase in fluorescence intensity was observed and subsequent calibration again indicated transfer of 60–70% (Figure 4B). This demonstrates that spontaneous flip-flop of Nod factors between inner and outer leaflets of membranes is prohibited. For transbilayer exchange (flip-flop), the bulky hydrophilic chitin moiety has to pass the hydrophobic lipid interior of the membrane. Apparently, this transition is highly unfavored and requires a high activation energy like that observed for lipids with a bulky polar headgroup (37, 38).

Transfer of Fluorescent Nod Factors from Vesicles to Root Hairs. To examine whether the Nod factors can transfer

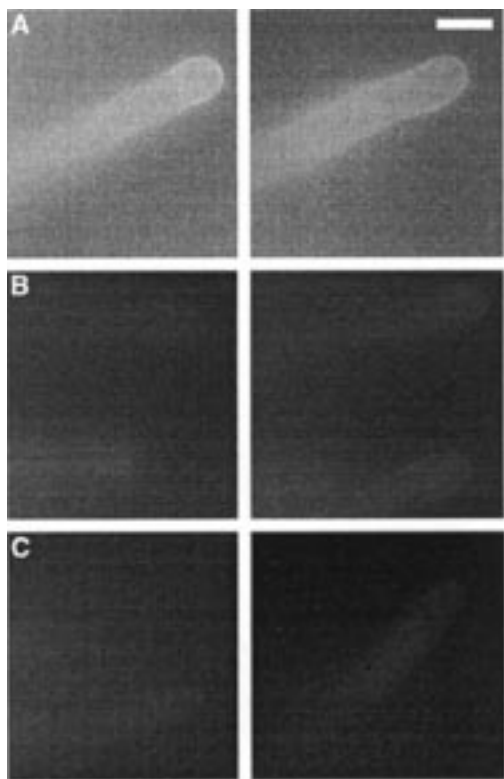


FIGURE 5: Images of *V. sativa* (vetch) root hairs, showing the fluorescence after incubation with quenched vesicles containing BODIPY-labeled Nod factors or phospholipids. All images are representative data of multiple (at least triplicate) experiments. Image exposure times, microscopy settings, and image processing (contrast stretching) were identical for all six subimages. The bar represents 15 μm . (A) Fluorescence of root hairs 10 min after incubation with quenched donor vesicles [79.4:10:10:0.6 DOPC/DPPA/Texas Red DHPE/NodRlv-IV(BODIPY FL-C₁₆), 100 nmol of total lipid in 1 mL of PGM without CaCl₂] containing Nod factor. (B) Fluorescence of root hairs 10 min after incubation with quenched donor vesicles (79.4:10:10:0.6 DOPC/DPPA/Texas Red DHPE/BODIPY FL DHPE, 100 nmol of total lipid in 1 mL of PGM without CaCl₂) containing a nontransferable lipid. (C) Autofluorescence of nontreated roots.

spontaneously from membranes (e.g., bacterial outer membranes) to the cell wall of root hairs, vesicles containing both NodRlv-IV(BODIPY FL-C₁₆) and the nonexchangeable quencher Texas Red DHPE were added to vetch roots on Fåhrus slides. To allow detection of NodRlv-IV(BODIPY FL-C₁₆) above the autofluorescence of the root hairs, a concentration of 0.6 μM was used, and a band-pass emission filter was employed excluding Texas Red fluorescence.

After application of the vesicles, this resulted in an increase of green fluorescence of the cell wall of the root hairs, as shown in Figure 5A. The labeling pattern is identical to the one observed when the Nod factors were added without vesicles (data not shown). Also, a clear Texas Red fluorescence could be observed at the root hair cell wall, indicating that at least part of the vesicles that are applied adhere at the root hair surface. Three hours after addition of the vesicles, root hairs were deformed normally, indicating that Nod factor perception is not different when Nod factors are administered as monomers or as vesicle-bound structures. In a control experiment, the BODIPY FL-labeled Nod factor was replaced by BODIPY FL DHPE (a nonexchangeable phospholipid). After addition of these vesicles (Figure 5B), the green fluorescence intensity of the root hairs was similar

to the root hair autofluorescence intensity detected on untreated plants (compare with Figure 5C), but a distinct Texas Red fluorescence signal could also be observed at the root hair surface (data not shown). This indicates that the increase in NodRlv-IV(BODIPY FL-C₁₆) fluorescence as shown in Figure 5A truly reflects desorption of Nod factor monomers from (adhered) vesicles and transfer to the root hairs, and not association or disintegration of vesicles at the cell wall. Given the comparable physicochemical properties of all four fluorescent Nod factors in relation to membranes, the results of the transfer experiments performed with NodRlv-IV(BODIPY FL-C₁₆) are most likely representative of the other fluorescent Nod factors and, moreover, naturally occurring Nod factors.

DISCUSSION

In this study, the behavior of fluorescently labeled Nod factors was investigated. The capability to deform root hairs of *V. sativa* seedlings was used to evaluate their bioactivity. It appears that the introduction of the hydrophobic BODIPY moieties at carbon atom C₁₆ of the fatty acyl chain does not seriously interfere with perception efficiency. This makes us feel confident that these fluorescent Nod factors can be used as truthful representatives of their natural counterparts, also in other systems.

Since Nod factors are amphiphilic molecules, with an acyl chain of 16 or more carbon atoms, special attention was given to their properties in the presence of membranes. No transbilayer movement of the Nod factors is observed within 15 h. In view of the cytoplasmic localization of the enzymes involved in the Nod factor biosynthesis in rhizobia (42–44), the inability of Nod factors to flip-flop spontaneously has direct implications for the bacterial Nod factor-secretion mechanism. Our observations imply that after biosynthesis in the cytoplasm, the Nod factors are trapped in the inner leaflet of the inner membrane of the bacterium. As a consequence, for enabling bacterial Nod factor secretion, there is an absolute requirement for a transfer mechanism in both bacterial membranes to effectively move Nod factors from the inner leaflet of the inner membrane to the outer leaflet of the outer membrane, e.g., an ATP-dependent flippase-like transport system (reviewed for aminophospholipids in ref 45). Indeed, three rhizobial proteins have been identified (NodI, NodJ, and NodT) which enhance secretion of Nod factors, but are not involved in the Nod factor biosynthesis (46, 47). For flippase activity, NodI is the most probable candidate, given its membrane association and ATP binding motif (47, 48). Further studies using model membranes containing NodI and fluorescent Nod factor as described here can determine whether these enzymes act as flippases.

FCS and time-correlated fluorescence spectroscopy revealed that, at 10⁻⁸ M, the fluorescent Nod factors are present as monomers in buffer and do not have the tendency to aggregate in micelles. We did not investigate whether Nod factors do form micelles at higher concentrations, but given the fact that Nod factors can elicit responses in legume root hairs at concentrations down to 10⁻¹² M (3, 10), we can exclude the possibility that formation of micellar structures by Nod factors is part of a biological activation mechanism at physiological concentrations. All four Nod factors have a

high tendency to insert in exogenously applied micelles or vesicles. From this, it is concluded that the physicochemical properties of the fluorescent Nod factors are quite similar, irrespective of the distinct differences in bioactivity (ref 8 and Table 1).

The transfer experiments show that NodRlv-IV(BODIPY FL-C₁₆) is able to redistribute between outer leaflets of different vesicles very rapidly. Although we did not perform detailed kinetic studies, we hypothesize that like the well-studied spontaneous transfer of short acyl chain phospholipids between membranes, the transfer mechanism involves desorption of monomers from the outer membrane leaflet (37–39, 49). This view is supported by the *in vivo* transfer experiments which showed that the Nod factors are able to desorb from vesicles to diffuse to the cell wall of root hairs, without significant fusion or disintegration of the vesicles. Given the observations, we postulate that Nod factors also will be able to spontaneously diffuse from the outer membrane of *Rhizobium* bacteria to the root hair cell wall and cell membrane, without the bacterium needing to provide a specific mechanism for enhancing desorption of Nod factor monomers from the bacterial outer membrane. This again supports our notion that the *nod* gene products indicated to be involved in rhizobial Nod factor secretion (46, 47) are involved in intrabacterial transbilayer transport of Nod factors.

In conclusion, we have shown that Nod factors are water soluble at physiological concentration, insert in membranes but are not able to flip-flop between membrane leaflets, and spontaneously transfer from membranes to legume root hairs. These observations provide novel and direct insight into how Nod factors behave in the presence of biomembranes and root hairs which increased our level of understanding of the mode of secretion and transfer of Nod factors during the early steps of the *Rhizobium*–legume interaction.

ACKNOWLEDGMENT

We are grateful to Jürgen Schmidt and Michael John (Abteilung Genetische Grundlagen der Pflanzenzüchtung, Max-Planck-Institut für Züchtungsforschung, Köln, Germany) for their continuous interest and help in the synthesis of the fluorescent Nod factors.

REFERENCES

- Heidstra, R., and Bisseling, T. (1996) *New Phytol.* 133, 25–43.
- Long, S. R. (1996) *Plant Cell* 8, 1885–1898.
- Roche, P., Debellé, F., Maillat, F., Lerouge, P., Faucher, C., Truchet, G., Dénarié, J., and Promé, J.-C. (1991) *Cell* 67, 1131–1143.
- Price, N. P. J., Relic, B., Talmont, F., Lewin, A., Promé, D., Pueppke, S. G., Maillat, F., Dénarié, J., Promé, J.-C., and Broughton, W. J. (1992) *Mol. Microbiol.* 6, 3575–3584.
- Lerouge, F., Roche, P., Faucher, C., Maillat, F., Truchet, G., Promé, J. C., and Dénarié, J. (1990) *Nature* 344, 781–784.
- Spaink, H. P., Sheely, D. M., van Brussel, A. A. N., Glushka, J., York, W. S., Tak, T., Geiger, O., Kennedy, E. P., Reinhold, V. N., and Lugtenberg, B. J. J. (1991) *Nature* 354, 125–130.
- Nicolaou, K. C., Bockovich, N. J., Carnague, D. R., Hummel, C. W., and Even, L. F. (1992) *J. Am. Chem. Soc.* 114, 8701–8702.
- Gadella, T. W. J., Jr., Vereb, G., Hadri, A.-E., Röhrig, H., Schmidt, J., John, M., Schell, J., and Bisseling, T. (1997) *Biochem. J.* 72, 1986–1996.
- Ehrhardt, D. W., Atkinson, E. M., and Long, S. R. (1992) *Science* 256, 998–1000.
- Heidstra, R., Geurts, R., Franssen, H., Spaink, H., van Kammen, A., and Bisseling, T. (1994) *Plant Physiol.* 105, 787–797.
- Van Brussel, A., Bakhuizen, R., van Spronsen, P., Spaink, H., Tak, T., Lugtenberg, B., and Kijne, J. (1992) *Science* 257, 70–72.
- Truchet, G., Roche, P., Lerouge, P., Vasse, J., Camut, S., de Billy, F., Promé, J.-C., and Dénarié, J. (1991) *Nature* 351, 670–673.
- Niebel, A., Bono, J.-J., Ranjeva, R., and Cullimore, J. V. (1997) *Mol. Plant-Microb. Interact.* 10, 132–134.
- Orgambide, G. G., Lee, J., Hollingsworth, R. I., and Dazzo, F. B. (1995) *Biochemistry* 34, 3832–3840.
- Rigler, R. (1995) *J. Biotechnol.* 41, 177–186.
- Maiti, S., Haupts, U., and Webb, W. W. (1997) *Proc. Natl. Acad. Sci. U.S.A.* 94, 11753–11757.
- Folch, J., Lees, M., and Sloane-Stanley, G. H. (1957) *J. Biol. Chem.* 226, 497–509.
- Bhuvanewari, T. V., and Solheim, B. (1985) *Physiol. Plant.* 63, 25–34.
- Van Brussel, A. A. N., Zaat, S. A. J., Canter Cremers, H. C. J., Wijffelman, C. A., Pees, E., Tak, T., and Lugtenberg, B. J. J. (1982) *Plant Sci. Lett.* 27, 317–325.
- Batzri, S., and Korn, E. D. (1973) *Biochim. Biophys. Acta* 298, 1015–1019.
- Hink, M. A., and Visser, A. J. W. G. (1998) in *Applied fluorescence in chemistry, biology and medicine* (Rettig, W., Strehmel, B., Schrader, S., and Seitert, H., Eds.) pp 101–118, Springer-Verlag, Berlin.
- Hink, M. A., Van Hoek, A., and Visser, A. J. W. G. (1999) *Langmuir* 15, 992–997.
- Rigler, R. J., Widengren, J., and Mets, Ü. (1992) in *Fluorescence spectroscopy* (Wolfbeis, O. S., Ed.) pp 13–24, Springer-Verlag, Berlin.
- Edward, J. T. (1970) *J. Chem. Educ.* 47, 261–270.
- Van Hoek, A., and Visser, A. J. W. G. (1992) *Proc. SPIE-Int. Soc. Opt. Eng.* 1640, 325–329.
- Van den Berg, P. A. W., Van Hoek, A., Walentas, C. D., Perham, R. N., and Visser, A. J. W. G. (1998) *Biophys. J.* 74, 2046–2058.
- Beechem, J. M., Gratton, E., Ameloot, M., Knutson, J. R., and Brand, L. (1992) in *Topics in Fluorescence Spectroscopy* (Lakowicz, J. R., Ed.) pp 241–305, Plenum Press, New York.
- Marquardt, D. W. (1963) *J. Soc. Ind. Appl. Math.* 11, 431–441.
- Johnson, I. D., Kang, H. C., and Haugland, R. P. (1991) *Anal. Biochem.* 198, 228–237.
- Philip-Hollingsworth, S., Dazzo, F. B., and Hollingsworth, R. I. (1997) *J. Lipid Res.* 38, 1229–1241.
- Haugland, R. P. (1996) *Handbook of molecular probes and research chemicals*, 6th ed., Molecular Probes Inc., Eugene, OR.
- Kinosita, K., Jr., Kawato, S., and Ikegami, A. (1977) *Biophys. J.* 20, 289–305.
- Kawato, S., Kinosita, K., Jr., and Ikegami, A. (1977) *Biochemistry* 16, 2319–2324.
- Struck, D. K., Hoekstra, D., and Pagano, R. E. (1981) *Biochemistry* 20, 4093–4099.
- Nichols, J. W., and Pagano, R. E. (1982) *Biochemistry* 21, 1720–1726.
- Van Paridon, P. A., Gadella, T. W. J., Jr., Somerharju, P. J., and Wirtz, K. W. A. (1988) *Biochemistry* 27, 6208–6214.
- Homan, R., and Pownall, H. J. (1988) *Biochim. Biophys. Acta* 938, 155–166.
- Bai, J., and Pagano, R. E. (1997) *Biochemistry* 36, 8840–8848.
- Nichols, J. W., and Pagano, R. E. (1981) *Biochemistry* 20, 2783–2789.
- Johnson, S. M., Bangham, A. D., Hill, M. W., and Korn, E. D. (1971) *Biochim. Biophys. Acta* 233, 820–826.
- Gadella, T. W. J., Jr., and Wirtz, K. W. A. (1994) *Eur. J. Biochem.* 220, 1019–1028.

42. Schlaman, H. R. M., Okker, R. J. H., and Lugtenberg, B. J. J. (1990) *J. Bacteriol.* 172, 5486–5489.
43. Barny, M. A., and Downie, J. A. (1993) *Mol. Plant-Microb. Interact.* 6, 669–672.
44. Bloemberg, G. V., Thomas-Oates, J. E., Lugtenberg, B. J. J., and Spaink, H. P. (1994) *Mol. Microbiol.* 11, 793–804.
45. Devaux, P. F. (1992) *Annu. Rev. Biophys. Biomol. Struct.* 21, 417–439.
46. Rivilla, R., Sutton, J. M., and Downie, J. A. (1995) *Gene* 161, 27–31.
47. Spaink, H. P., Wijfjes, A. H. M., and Lugtenberg, B. J. J. (1995) *J. Bacteriol.* 177, 6276–6281.
48. Downie, J. A. (1998) in *The Rhizobiaceae-Molecular Biology of model plant-associated bacteria* (Spaink, H. P., Kondorosi, A., and Hooykaas, P. J. J., Eds.) pp 387–402, Kluwer, Dordrecht, The Netherlands.
49. Roseman, M. A., and Thompson, T. E. (1980) *Biochemistry* 19, 439–444.

BI990714Q